and integrating both sides leads to

$$e^{\beta R(t)} - e^{\beta R(0)} = -\alpha t \tag{2.2.14}$$

Once $R(t) \to 0$, then the size of the central domain $2R \to 0$ and it means that the kink and the anti-kink disappear simultaneously: this is known in physics as **annihilation**. So the time it takes for the couple to annihilate, can be calculated requiring that $R(t) = 0$

$$\tau_{annhilation} = \frac{1}{\alpha}(e^{\beta R(0)} - 1) \sim e^{\beta R(0)} \tag{2.2.15}$$

The time needed for a couple of neighbouring kink and anti-kink to annhilate grows exponentially with their distance. Due to this mechanism, some domains disappear and so the others grow as an effect of the fixed size of the system. The increase of the typical size of domains as time passes is known as **coarsening** in the literature. Even if the state is less-trivial than Eq. 2.2.10, so if there are many domains, their typical size ℓ grows very slowly in time as a consequence of the long annhilation times

$$\ell(t) \sim \log t \tag{2.2.16}$$

Unfortunately, it is difficult to check numerically that the domain size grows respecting this law. The reason is that a logarithmic growth is very slow and so a very long computational time is needed to verify this law.

2.3 The 2D dynamics

In the previous section, we examined the dynamics governed by the 1D Time-Dependent Ginzburg-Landau (TDGL) equation, focusing on solutions along a single spatial dimension $x \in \mathcal{R}$. Now, we turn our attention to the **2D** TDGL equation, where the spatial coordinate $\mathbf{x}$ describes a point in a plane $(x, y) \in \mathcal{R}^2$. The TDGL equation for this two-dimensional case is:

$$\partial_t m = \Delta m + Cm - m^3 \quad \text{where} \quad \Delta = \partial_{xx} + \partial_{yy} \tag{2.3.1}$$

Just as in the 1D case, if the initial state is a small perturbation of zero, there is a linear instability that determines the initial dynamics. This instability leads to the formation of domains, where $m(x, y) = \pm\sqrt{C}$ (Figure 2.6). The interfaces between these domains are now curves in the (x, y) plane, and along a line perpendicular to an interface, the shape resembles that of the 1D kink solutions up to leading order. The key difference in 2D lies in the dynamics of these interfaces, determined by the non-linear part of the equation. Specifically, the interfaces evolve according to a mechanism known as *motion by curvature*. In this context, each point on an interface moves with a velocity perpendicular to the interface and proportional to the local curvature. This mechanism leads to coarsening dynamics, where the characteristic size of domains ℓ grows as a power law of time, $\ell(t) \sim t^{\frac{1}{2}}$, independently on the value of C. This growth is significantly faster than in the 1D case, where the domain sizes could be considered effectively frozen after the linear dynamics.

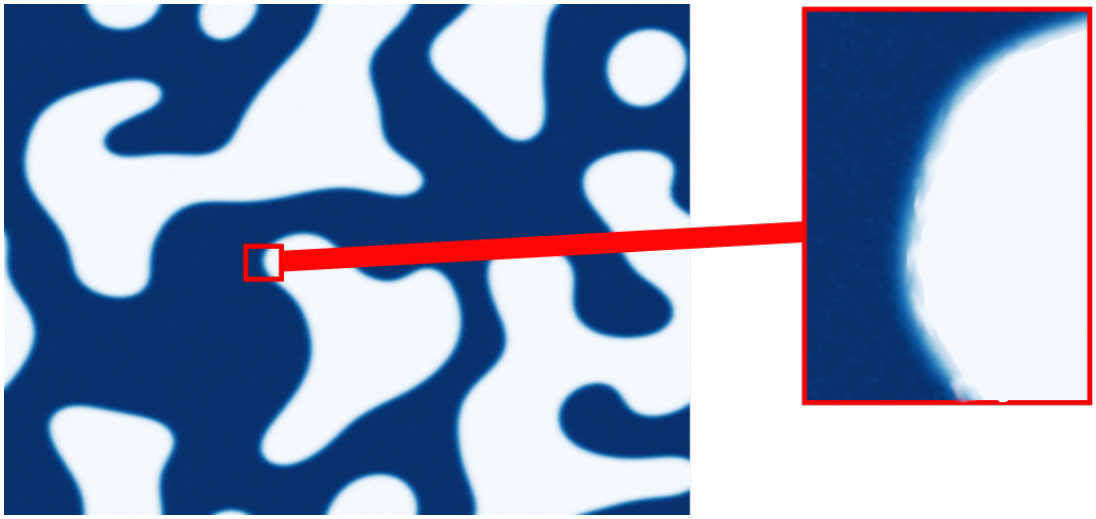

Figure 2.6: On the left: Simulation of the 2D TDGL equation (Eq. 2.3.1) until a long time after the initial linear instability, such that we can study the asymptotic dynamics, when domains are already formed. White regions represent domains where $m(x, y) = -\sqrt{C}$, while in the blue regions $m(x, y) = +\sqrt{C}$. On the right: Zoom of a region of the interface between two neighbouring domains.

As an example, we will show simulations of the 2D TDGL equation with an initial state comprising an *isolated circular domain*. We will see that the domain shrinks in time with the speed predicted by motion by curvature. We will also make use of simulations to compare the speed of coarsening dynamics between the 1D and 2D cases, highlighting the essential differences in domain growth rates.

2.3.1 The new leading mechanism for the dynamics: motion by curvature

In the following section, we will demonstrate that the dynamics of an interface is primarily governed by its curvature. To achieve this, we will first introduce a new coordinate system $(x, y) \to (\xi, s)$ that is more naturally suited for describing the dynamics of the interface.
After establishing the new coordinate system, we will make some empirical observations about the asymptotic dynamics of the system. These observations will be used as assumptions, forming the basis for our proof that the interface motion is driven by curvature.

A new coordinate system

We can formally define an **interface** as a curve in the plane where the order parameter $m(x, y)$ is constant and equal to zero (Figure 2.7a). This curve represents the boundary between two neighbouring domains, where $m(x, y)$ takes on different values: $\pm\sqrt{C}$. To describe the dynamics of the interface, we'll switch from Cartesian coordinates (x, y) to a more natural coordinate system (ξ, s) relative to the interface. In this new coordinate system:

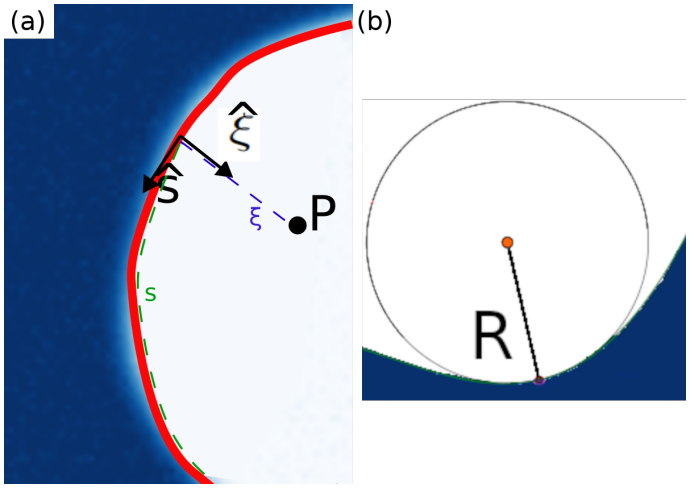

Figure 2.7: (a) Interface between two domains (Figure 2.6). In red is highlighted the interface between two domains, that is the curve where $m(x, y) = 0$. The position of the point P is described by its distance from the interface ξ (in blue) and the position of its projection along the interface s (in green). (b) Circle tangent to the interface at a point P. If R is its radius, then $\kappa = R^{-1}$ is the curvature of the interface at the point P.

- ξ represents the distance of the point P from the interface along the direction normal to the interface.
- s represents the position of the projection of the point P onto the interface. Equivalently, if you take the curve of points with an equal distance $\xi = \bar{\xi}$ from the interface, then s is the coordinate distinguishing the point in this curve.

Since the interface is a curve within the plane, we can define the local **curvature** κ at any given point along the interface. The *modulus* of the curvature κ is mathematically defined as:

$$|\kappa| = \frac{1}{R}$$

Here, R represents the radius of the osculating circle that is tangent to the interface at that specific point, as shown in Figure 2.7b. The modulus $|\kappa|$ quantifies the degree of bending of the interface: a larger curvature indicates a sharper bend (smaller R), while a smaller curvature indicates a more gradual bend or even a flat region (larger R). In 2D, the curvature has a *sign*. Since the unit vector $\hat{\xi}$ must vary smoothly along the interface, it cannot be defined as pointing toward the center of the tangent circle at every point of the interface. Consequently, $\hat{\xi}$ may point either toward the center of the tangent circle or in the opposite direction, resulting in the curvature κ being either negative or positive, as shown in Figure 2.8.

Motion by curvature

During the asymptotic dynamics, simulations show that the curvature of the interfaces is small compared to the *thickness of the interface*, defined as the length of the

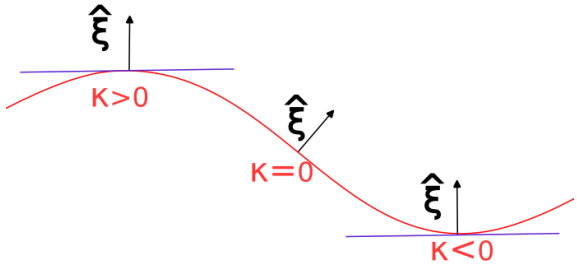

Figure 2.8: The interface (shown in red) is a curve that divides the plane into two regions. At any point along the interface, we can draw a tangent line (shown in blue) and define the "exterior" of the curve as the region where the tangent lies, with the "interior" being the opposite region. Since the unit vector $\hat{\xi}$ can point either toward the interior or exterior, we can introduce the concept of the *sign* of the curvature. We define the curvature as $\kappa > 0$ when $\hat{\xi}$ points toward the exterior of the curve and $\kappa < 0$ when it points toward the interior. At points where the curve is flat (to leading order), this distinction is not possible, consistently with the fact that $|\kappa| = 0$ at such points.

region where $\partial_\xi m$ is significantly different from zero. Additionally, the curvature changes gradually along the interface (as illustrated in Figure 2.6).
The aim of this section is to formalize these empirical observations into assumptions and to prove that the dynamics of the interface is predominantly governed by its curvature, through a mechanism known as **motion by curvature**.
As the existence of the concept of curvature distinguishes the 2D case from the 1D one, we expect that if the curvature is small, the system will exhibit properties similar to those discussed for a 1D system. Specifically, along the direction $\hat{\xi}$, which is orthogonal to the interface, the shape of the interface should resemble that of the 1D kink solutions. This implies that if we consider the curve of points characterized by the same $\xi = \bar{\xi}$ (a curve of points at the same distance from the interface), it will be well approximated by a curve where m is constant. Consequently, m will vary slowly with respect to s. Additionally, since the length of a 1D kink is approximately $\sim C^{-\frac{1}{2}}$, choosing $\mathbf{C} \sim \mathbf{1}$ leads us to conclude that the thickness of the 2D interfaces is also of order ~ 1.
As a consequence of the previous considerations, we can formalize our assumptions as

- κ is small compared with the interface width (~ 1)

$$\kappa = \epsilon_1 K_1 \quad \text{where: } K_1 \sim 1; \quad \epsilon_1 << 1 \tag{2.3.2}$$

- $m(\xi, s)$ depends slowly on s

$$\delta m \sim \epsilon_2 \quad \text{if } \delta_s \sim 1 \quad \text{where: } \epsilon_2 << 1$$

while

$$\delta_m \sim 1 \quad \text{if } \delta\xi \sim 1$$

that can be re-stated as

$$\partial_s m = \epsilon_2 \partial_\xi m \tag{2.3.3}$$

In addition to assumptions 2.3.2 and 2.3.3, we assume that the shape of the interface remains constant during the time it takes for the interface to propagate over a distance of order 1, which is the order of magnitude of the thickness of the interface. Furthermore, we assume the speed v of the interface to be slow, meaning that a considerable amount of time is required for the interface to traverse a length of order 1. Formalizing the last assumptions, we find the properties

$$m(\xi, s, t) = m(\xi - vt, s, 0) \implies \partial_t m = -v\partial_\xi m \tag{2.3.4}$$

$$v = \epsilon_3 V_1 \quad \text{where: } V_1 \sim 1, \epsilon_3 << 1 \tag{2.3.5}$$

Before employing the stated assumptions to demonstrate that curvature drives the dynamics of the interfaces, we notice that we introduced the presence of three *different* small parameters, denoted as ϵ_i. To simplify our analysis, we can invoke an additional assumption known in the literature as the **scaling hypothesis**. This means assuming that all large-scale features of the system are characterized by the same length scale ℓ. This implies that these features are of the same order, leading to the relationship:

$$\epsilon_1 = \epsilon_2 = \epsilon_3 = \epsilon$$

It is important to note that this holds true only for large-scale features, as there is clearly another scale present in the system: the thickness of the interface, which is a short-scale feature.
We're finally able to use the stated assumptions 2.3.2, 2.3.3, 2.3.4 and 2.3.5 in the TDGL equation, along with the expression for Δ in the coordinates (ξ, s), that is calculated in Appendix D

$$\Delta = \frac{\kappa}{1+\xi\kappa}\partial_\xi + \partial_{\xi\xi} + \frac{1}{1+\xi\kappa}\partial_s\left(\frac{1}{1+\xi\kappa}\partial_s\right)$$

By using the assumptions 2.3.2 and 2.3.3, up to leading order in ϵ

$$\Delta = \partial_{\xi\xi} + \epsilon K_1 \partial_\xi + O(\epsilon^2) \tag{2.3.6}$$

Recalling the TDGL equation

$$\partial_t m = \Delta m + Cm - m^3$$

and using 2.3.4, 2.3.5 and 2.3.6, we find at leading order in ϵ

$$-\epsilon V_1 \partial_\xi m = \partial_{\xi\xi} m + \epsilon K_1 \partial_\xi m + Cm - m^3 \tag{2.3.7}$$

Then it is natural to expand also the order parameter in powers of ϵ

$$m = m_0 + \epsilon m_1 + O(\epsilon^2)$$

Equating the terms of order zero (ϵ^0), we find

$$\partial_{\xi\xi} + Cm_0 - m_0^3 = 0 \tag{2.3.8}$$

that is the Eq. 2.2.3 where $x \to \xi$, so we already know the solution

$$m_0(\xi, t) = C(t)^{\frac{1}{2}} \tanh\Big(\xi C(t)^{\frac{1}{2}} 2^{-\frac{1}{2}}\Big)$$

Up to order zero, the shape of the interface along the direction $\hat{\xi}$ is the same of a 1D kink (Eq. 2.2.9). While equating the terms of order ϵ, we find a less trivial result

$$(\partial_{\xi\xi} + C - 3m_0^2)m_1 = -(V_1 + K_1)\partial_\xi m_0 \tag{2.3.9}$$

We could not figure out how to solve this equation for m_1. However it's possible to use a theorem known as the *Fredholm alternative* (and proved in Appendix E) to find a relation between the parameters of the equation (C, V_1, K_1). The theorem states that, given a solution $u(\xi)$ of the in-homogeneous differential equation Eq. 2.3.9 and an homogeneous solution $v(\xi)$

$$\hat{L}u(\xi) = f(\xi)$$
$$\hat{L}v(\xi) = 0$$

where

$$\hat{L} = (\partial_{\xi\xi} + C - 3m_0^2)$$
$$f(\xi) = -(V_1 + K_1)\partial_\xi m_0$$

then

$$\int_{-\infty}^{+\infty} f(\xi)v(\xi)d\xi = [\partial_\xi uv - u\partial_\xi v]_{-\infty}^{+\infty} \tag{2.3.10}$$

We can use this mathematical theorem to retrieve some information from Eq. 2.3.9. The in-homogeneous solution is $u = m_1$ then, deriving Eq. 2.3.8 respect to ξ

$$\partial_{\xi\xi}(\partial_\xi m_0) + C\partial_\xi m_0 - 3m_0^2\partial_\xi m_0 = 0$$

so $v(\xi) = \partial_\xi m_0$ is an homogeneous solution ($\hat{L}u(\xi) = 0$) and we can apply the theorem 2.3.10

$$-(V_1 + K_1)\int_{-\infty}^{+\infty} (\partial_\xi m_0)^2 d\xi = 0$$

where in the last equation we assumed that the right side of Eq. 2.3.10 is zero. As the integral is non-zero, it means that

$$V_1 = -K_1$$

So an interface moves with a velocity orthogonal to itself and it's proportional to the curvature κ. This effect is called **motion by curvature**

$$v = \epsilon V_1 = -\epsilon K_1 = -\kappa \tag{2.3.11}$$

The dynamics of an interface is, up to leading order in ϵ, governed by the curvature κ and the velocity v does not depend on the parameter C.
This result is consistent with the fact that v represents the velocity at which the interface propagates along the direction of $\hat{\xi}$. Indeed, $\hat{\xi}$ can point either inward or outward relative to the interface, but in both cases, the sign of the curvature changes accordingly, ensuring that the velocity always points toward the interior of the curve.

Figure 2.9: Schematic for the dynamics of the interfaces in 2D. The interface moves with a velocity $v = -\kappa$ where κ is the local curvature (Fig. 2.7b).

Example: isolated circular domain

The simplest way for verifying that motion by curvature (Eq. 2.3.11) is the leading mechanism of the dynamics, is studying a simulation of the 2D TDGL equation considering as the initial state an isolated circular domain of radius R_0 (Figure 2.10).
The initial state is set up as follows:

$$m(t=0) = \sqrt{C}\tanh\left(\sqrt{\frac{C}{2}}(r - R_0)\right)$$

where

$$r = \sqrt{x^2 + y^2}.$$

To measure the radius as a function of time $R(t)$, we calculate the average of the radial coordinate r weighted by the squared gradient of the order parameter $|\nabla m|^2$:

$$R^2(t) = \frac{\int r^2 |\nabla m|^2 \, dx \, dy}{\int |\nabla m|^2 \, dx \, dy}.$$

This method is expected to provide a good estimate of the radius of the circular island since $|\nabla m|^2$ is sharply peaked at the interface and nearly zero elsewhere.
In the case of a circular interface, the curvature κ is the same at any point and $\kappa = \frac{1}{R}$, where R is the radius of the circular domain. This means that the velocity of the interface $v = \dot{R}$ satisfies

$$\dot{R} = -R^{-1}$$

and so

$$R^2(t) = R_0^2 - 2t \tag{2.3.12}$$

so the area of the domain ($2\pi R^2$) shrinks linearly in time, until it disappears. In Figure 2.10 this behaviour is verified in a simulation, confirming that motion by curvature is the leading mechanism determining the dynamics in a 2D system.

2.3.2 Coarsening

In 2D, the concept of curvature fundamentally alters the dynamics of the interfaces. However, similar to the 1D case, this curvature-driven dynamics leads to coarsening,

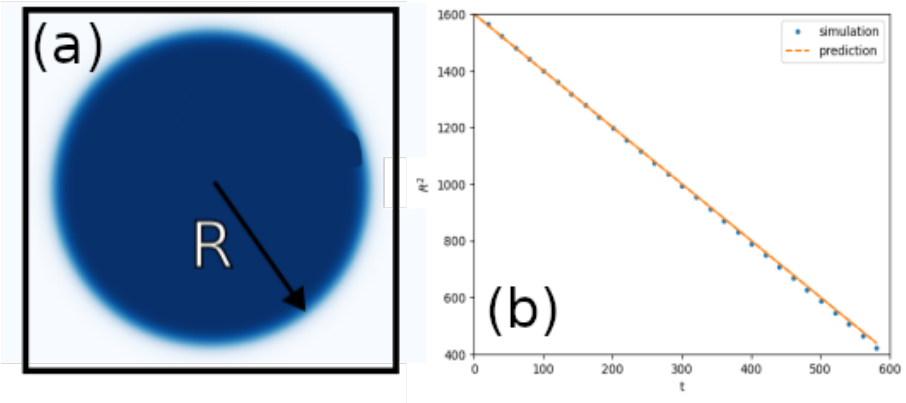

Figure 2.10: (a) Isolated circular domain with radius R. (b) Measure of $R^2(t)$ in a simulation of the 2D TDGL where the initial state is prepared as (a). $C = 0.5, R_0 = 40, L = 128, dt = 0.1$.

the size of the domains increases over time. In two dimensions, the coarsening process is significantly faster: the typical size of the domains scales with time as a power law, specifically $\ell \sim t^{\frac{1}{2}}$. In contrast, in 1D, the scaling is logarithmic, $\ell \sim \log t$, which results in domains that can be considered effectively frozen.
To demonstrate this result, we will employ a dimensional analysis, which is not applicable in the 1D case as it makes use of the motion by curvature $v = -\kappa$ relation. Dimensional $[v] = \frac{[L]}{[t]}$, where v is the interface velocity and $[L], [t]$ represent respectively a length and a time. Then motion by curvature tells that $v = -\kappa$ and $[\kappa] = \frac{1}{[L]}$. Together the relations tell that $1/L \sim L/t$ so

$$\ell(t) \sim t^{\frac{1}{2}} \tag{2.3.13}$$

where $\ell(t)$ is a length-scale describing the size of the domains.
To verify this coarsening law numerically, we need to define a measurable quantity that describes the typical size of the domains. The idea we propose is to consider the function $|\nabla m|^2$ as this function will be significantly different from zero only where there is an interface. In 1D, we can define this length-scale

$$\ell_{DW} = \frac{L}{\int (\partial_x m(x))^2 dx} \int (\partial_x m_0(x))^2 dx \tag{2.3.14}$$

where L is the size of the system (of the simulation box), while m_0 is the stationary state with only one kink, that is defined in Eq. 2.2.9. As the shape of the kinks is the same for each kink and it is defined by Eq. 2.2.9, then the ratio $N = \frac{\int (\partial_x m(x))^2 dx}{\int (\partial_x m_0(x))^2 dx}$ corresponds to the number of kinks. As a consequence, $\ell_{DW} = L/N$ is the average size of a 1D domain.
Then we can extend the definition of ℓ_{DW} to the 2D case

$$\ell_{DW} = \frac{L^2}{\int |\nabla m(x)|^2 dx dy} \int (\partial_x m_0(\xi))^2 d\xi \tag{2.3.15}$$

where we still consider ℓ_{DW} as a measure of the typical size of the domains.

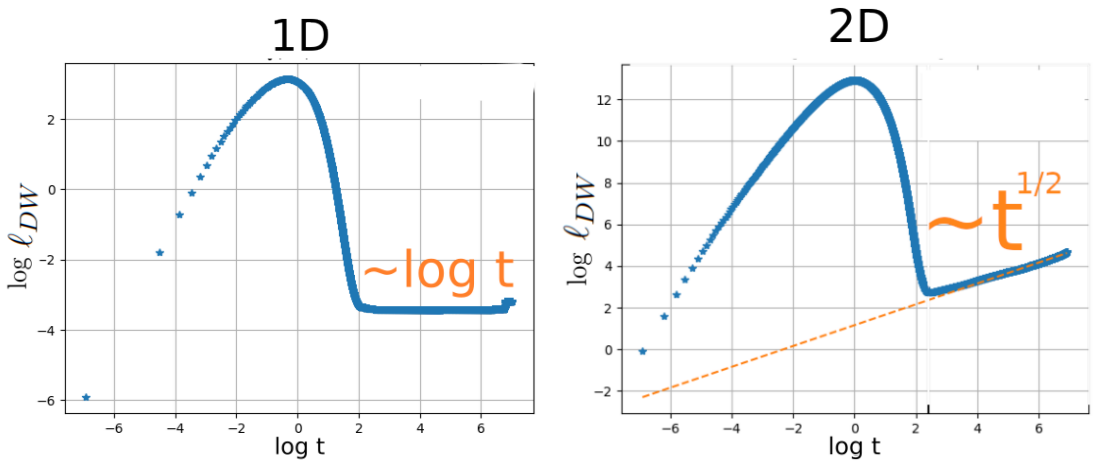

Figure 2.11: Simulations of the 1D and 2D TDGL equations, starting from an initial state that is a small perturbation of zero in both cases. The typical domain size, ℓ_{DW}, is measured as a function of time. The expected coarsening laws, $\ell_{1D} \sim \log t$ for the 1D case and $\ell_{2D} \sim t^{\frac{1}{2}}$ for the 2D case, are verified at long times in the log log scale plots. In the 1D simulation, we would need a much longer duration to observe the expected logarithmic relationship clearly. In shorter simulations, the size of the domains appears frozen. At very early times, domains have not yet formed, meaning that ℓ_{DW} does not accurately represent the size of the domains. During the linear dynamics, we used a time step of $dt = 0.001$ to precisely capture the domain formation process up to time $t = 8$. Following this, we switched to a larger time step of $dt = 0.1$ to simulate the slower coarsening dynamics.

In Figure 2.11 the coarsening laws for the 1D and the 2D cases are verified by simulating the 1D and the 2D TDGL equation for a long time and measuring $\ell_{DW}(t)$ as a function of time. The expected laws are verified only at long times, as at short times domains are not yet formed and so ℓ_{DW} is not a measure of the size of domains. Let's also notice that, as at long times the curvature of any interface is small, the shape of the interface along a perpendicular direction is well approximated by the 1D kink shape $m_0(\xi)$. As a consequence,

$$\int |\nabla m(x)|^2 dxdy \simeq \mathcal{L} \int (\partial_x m_0(\xi))^2 d\xi$$

where $\mathcal{L}$ is the sum of the lengths of all the interfaces. It follows that in 2D

$$\ell_{DW} = \frac{L^2}{\mathcal{L}}$$

meaning that the total length of the interfaces decreases in time, as ℓ_{DW} increases. And this is expected, as the number of domains decreases in time during coarsening dynamics.